

Synthesis and study of optical properties of microstructure flower-shaped ZnO

Rajat K. Saha, Eeshankur Saikia and Mrinal K. Debanath*

Department of Applied Sciences, Gauhati University, Guwahati, 781014, India

*Corresponding author

DOI: 10.5185/amlett.2018.2066

www.vbripress.com/aml

Abstract

In this study, we report the synthesis and optical properties of flower-shaped ZnO which is fabricated successfully using polyvinylpyrrolidone (PVP) as capping agent by wet chemical method at temperature 60°C. The structures and morphologies of flower-shaped ZnO is characterized by X-ray diffraction (XRD), Scanning Electron Microscopy (SEM), and Transmission Electron Microscopy (TEM) for nonlinear dynamical study of the system of particles. The studies of SEM and TEM have confirmed flower-shaped structure of the ZnO. The UV-vis absorption spectroscopy of the synthesized sample indicates the presence of blue shift. FTIR analysis shows the characteristic absorption of the Zn-O bond. It has been observed in room temperature photoluminescence (PL) spectroscopy of the sample exhibits emission peaks at near band edge (NBE) along with a weak blue emission peak. It is found from the present study that the phenomenon of flower-like microstructure is based on the size and shape of the particles as well as their aggregated forms. Moreover, their optical properties predict the factors responsible in inhibiting microorganisms for which it may lead to some biological applications. Copyright © 2018 VBRI Press.

Keywords: ZnO, flower-shaped, electron microscopy, growth, optical properties.

Introduction

In the last few decades, study of one dimensional (1D) materials has become a leading edge in nanoscience and nanotechnology. It has been reported by many researchers that growth of ZnO nanostructures in different shapes such as Nano rod [1], plates [2], nanotube [3], Nano belts [4], nanowire [5], hollow spheres [6], flower-like ZnO nanostructures [7-9], etc., has been synthesized by controllable morphology for exploring the potentials of ZnO nanostructures (NSs) due to its wide band gap (3.3 eV at 300 K) and a large exciton-binding energy (60 meV). In synthesis of ZnO nanoparticles (NPs), chemical capping method has been extensively used for controlling the particle sizes and also particles agglomeration [10, 11]. The particles of ZnO formed in Nano size have been studied for antibacterial activity with human pathogenic bacteria [12]. In this work, we report the formation of flower-shaped ZnO microstructure and its growth in PVP matrix. The optical properties, structures and morphologies have been investigated by using UV-vis absorption spectroscopy, PL spectroscopy, XRD, SEM, and TEM analyses. FTIR spectroscopy has been applied to perform a subtle analysis on structure formation of ZnO. The size is an eminent factor of the materials in inhibiting the microorganisms *Escherichia coli* and *Staphylococcus aureus* [13]. Flower-shaped ZnO NPs exhibit good antibacterial activities after UV illumination for a short time and also higher intensity of

PL in visible region increases the antibacterial effect of flower-shaped ZnO NPs [14]. The structure formation of the particles which is due to the presence of nonlinearity in the system can also be predicted by calculating one of the nonlinear dynamical (NLD) parameter which will be discussed in the next work to be reported.

Experimental

Materials

All materials were purchased from the commercial market and used without further purification. Zinc nitrate hex hydrate [$Zn(NO_3)_2 \cdot 6H_2O$] and ammonium hydroxide (NH_4OH) as the starting materials were purchased from Merck Specialties Private Limited, Mumbai, India, polyvinylpyrrolidone (PVP) as capping agent purchased from LOBA Cheme, Mumbai, India and double-distilled water as dispersing solvent was used to prepare flower-shaped ZnO purchased from Merck Specialties Private Limited, Mumbai, India.

Method

The synthesis of flower-shaped ZnO has been carried out by a simple wet chemical method reported earlier [15], except we have used 0.075 mol solution of $Zn(NO_3)_2 \cdot 6H_2O$ as a zinc source. 100 ml of 0.075 mol solution of $Zn(NO_3)_2 \cdot 6H_2O$ is stirred constantly for 30 minutes at 60°C (solution A). 3 wt% of PVP is stirred

constantly at 60°C for 30 minutes (solution **B**). Now NH_4OH was slowly added drop by drop into the solution **A** and stirred at room temperature for 15 minutes and the pH of the solution is continuously measured. When the pH of the solution is reached 7.5 and a white solution (solution **C**) of ZnO is formed then pouring of NH_4OH is stopped. The final mixture (solution **B** and solution **C**) is stirred constantly for 1 hour at 60°C and allowed to cool down at room temperature till the white precipitate of ZnO is formed. The whole solution is allowed to settle for overnight in a dark chamber. Finally, the precipitate is filtrated and washed with distilled water to dissolve the impurities and is dried at 60°C in oven for 12 hours.

Powder X-ray diffraction (XRD) pattern of prepared ZnO nanoparticle is recorded by Philips X-ray Diffractometer (X'Pert Pro) with $\text{Cu K}\alpha_1$ radiation ($\lambda = 1.5406 \text{ \AA}$). Field Effect Scanning Electron Microscope (MIRA3 TESCAN) and Transmission Electron Microscope (JEM-2100, Jeol) have been used for confirmation of flower-shaped ZnO microstructures. The optical absorption spectra of ZnO dispersed in water are recorded by a UV-vis spectrophotometer (HITACHI U - 3210). Room temperature PL and FTIR spectra are measured by using Fluorescence Spectrophotometer (HITACHI F-2500) at an excitation wavelength of 300 nm and PerkinElmer Fourier transform infrared spectrometer (Spectrum Two) in the range of 400 - 4000 cm^{-1} respectively.

Results and discussion

Fig. 1 shows the XRD profiles of the sample. The peaks correspond to (100), (002), (101), (102), (110), (103), (200), (112), and (201) planes that are well indexed *Powder Diffraction File* (PDF No. 36 - 1451), indicating hexagonal phase of ZnO with space group $\text{P6}_3\text{mc}$ (186). The crystallite size of the flower-shaped ZnO nanoparticles (NPs) are estimated for the preferred planes (hkl) using Debye Scherer's formula [16].

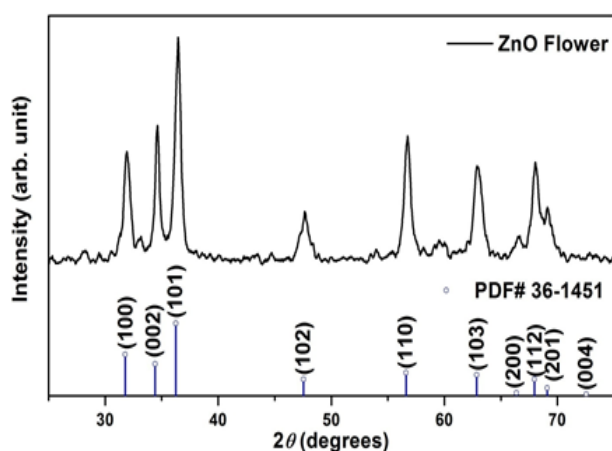


Fig.1. XRD profile of flower-shaped ZnO.

The average crystallite size is found to be $\sim 18.34 \text{ nm}$ in the directions perpendicular to (100), (002) and (101) planes. The ratio of the intensities of the XRD $I_{(002)}/I_{(101)}$ is found to be ~ 0.56 , which indicates that the preferred orientation of growth of the sample is along the (002) direction [7]. The material in Nano range had inhibited the bacteria in different amount, whose calibration with the Lyapunov Exponent is found suited for biological application [13].

While **Fig. 2(a) & (b)** show the SEM images, **Fig. 3(a)-(d)** show TEM images of the flower-shaped ZnO structures. The length of each petal is $\sim 0.8 - 0.9 \mu\text{m}$ as seen in SEM image and $\sim 0.9 - 0.95 \mu\text{m}$ in TEM image. All the petals have been originated from a center point of the flower-shaped ZnO microstructure having diameter $\sim 2 - 2.25 \mu\text{m}$ and $\sim 1.75 \mu\text{m}$ from SEM and TEM images respectively. In FESEM and HRTEM images shown in **Fig. 2(b)** and **3(d)**, all petals are aggregation of ZnO NPs of an average particle size less than $\sim 25 \text{ nm}$. The inter-planar spacing or d-spacing value is measured to be $\sim 0.26 \text{ nm}$, which corresponds to standard value for bulk ZnO along (002) direction (PDF No. 36-1451).

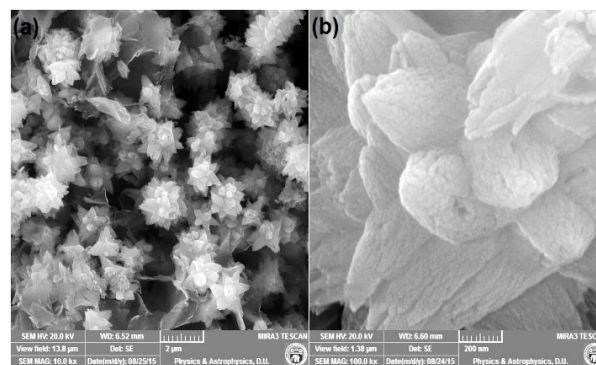


Fig. 2. FESEM images of (a) large area and (b) small area flower-shaped ZnO.

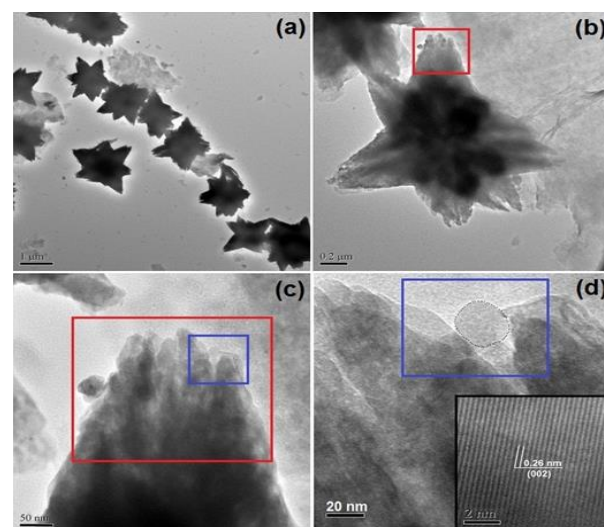
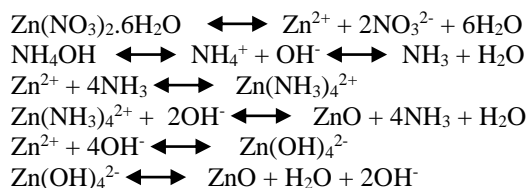


Fig. 3. HRTEM images of (a) large area TEM image, (b) TEM image of a single ZnO flower, (c) & (d) HRTEM images of the tip marked with red square and a blue square [inset of (d): lattice of ZnO flower] flower-shaped ZnO.

In our study, formation of ZnO is achieved via the wet chemical route, by the dehydration of $\text{Zn}(\text{OH})_4^{2-}$ or $\text{Zn}(\text{NH}_3)_4^{2+}$ according to the precursors reactions [11]:



The formation of ZnO were dependent on amount of solution pH and solvent used as reaction media which influenced the growth of ZnO structure as well as size and morphology of the nanoparticles [7, 11, 17]. At weak basic condition due to NH_3 and $\text{Zn}(\text{NH}_3)_4^{2+}$ with a low reaction temperature (60°C), more Zn^{2+} are transformed in the function of OH^- . Therefore, more ZnO aggregates spontaneously along active sites for the formation of flower-shaped ZnO microstructure. The morphologies of ZnO structures determined from $\text{Zn}(\text{OH})_4^{2-}$ plays an important role for controlling the growth of different crystal faces that lead to the formation of anisotropic structure like flower-shaped ZnO [8]. In addition, quartzite ZnO crystal is a polar crystal having a positive polar plane rich in Zn (0001), six symmetric nonpolar $\{10\text{-}10\}$ planes of the side facets and a negative polar plane rich in O (000-1) [18]. Different planes have different growth rates and are reported as $V_{(0001)} > V_{(10\text{-}11)} > V_{(10\text{-}10)} > V_{(000\text{-}1)}$ [19]. The negatively charged complex ions $\text{Zn}(\text{OH})_4^{2-}$ are preferentially adsorbed onto the positively charged Zn (0001) faces and subsequently dehydrate and enter into the crystal lattice favored greatly (0001) face for the growth [20]. However, capping agent PVP has a tendency to selectively adsorb on the $\{10\text{-}10\}$ planes of the six symmetric side facets of the growth nuclei, allowing occurred only along the polar axis [21].

In our investigation, PVP which is a water soluble polymer with both N and C=O groups, has been used as capping molecules and also acts as stabilizer against agglomeration. Fig. 4 shows amphiphilic structure of PVP molecules. The pyrrolidone part (hydrophilic) acted as head group while the polyvinyl part (hydrophobic) acted as tail group. The influence of PVP has not been restricted only to the solution but also affects the formation of the nuclei (*i.e.* nucleation) of the ZnO nanoparticles. That the particles prepared are in Nano range is also confirmed by HRTEM analysis [12].

In the presence of PVP, there exists a strong interaction between the surfaces of nanocrystals and PVP based strong coordination ability of O and N atoms in the pyrrolidone ring. So with the ZnO-PVP sample, it is believed that the bond between metal ions and PVP can give rise to overlapping of molecular orbital of PVP with atomic orbital of metal ions in surface regions. Therefore, we believe that the PVP passivating layers around the ZnO core shown in Fig. 4 are formed by coordination bonds between N atom of PVP and Zn^{2+} ion [22]. Thus PVP either controls the

growth of the particles by forming passivation layers around the ZnO core via coordination bond formation between the nitrogen atom of the PVP and Zn^{2+} ion, or it prevents agglomeration by steric effect due to the repulsive force acting among the polyvinyl groups (tail part). Therefore, the PVP encapsulation creates a restricted environment around the ZnO nanocrystals [23].

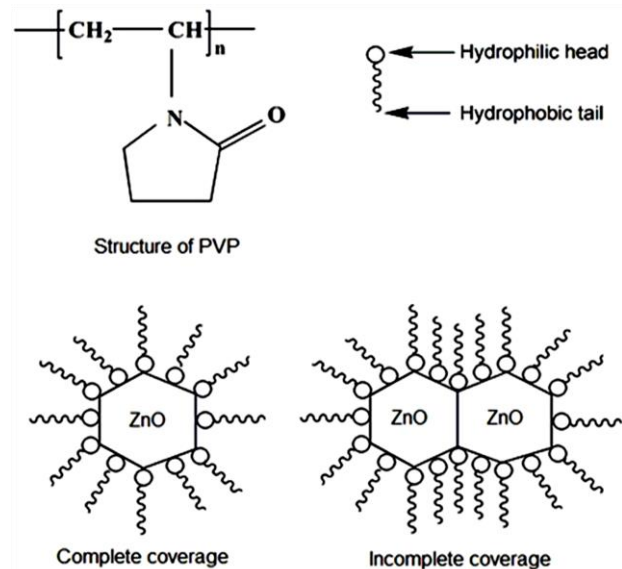


Fig. 4. Amphiphilic structure of PVP.

The UV absorption spectra in Fig. 5 shows absorption peak at $\lambda \sim 300$ nm (4.13 eV), which indicates the presence of blue shift with respect to bulk ZnO ($\lambda \sim 376$ nm; 3.3 eV) [15]. The direct band gap of flower-shaped ZnO shown in Fig. 5 inset has been estimated from the graph of $h\nu$ versus $(\alpha h\nu)^2$ for the absorption coefficient α , which is related to the band gap E_g as $(\alpha h\nu)^2 = k(h\nu - E_g)$, where $h\nu$ is the incident light energy and k is a constant. The extrapolation of the straight line in Fig. 5 inset to $(\alpha h\nu)^2 = 0$ gives the value of band gap energy E_g . The optical band gap value obtained for flower-shaped ZnO is ~ 3.781 eV.

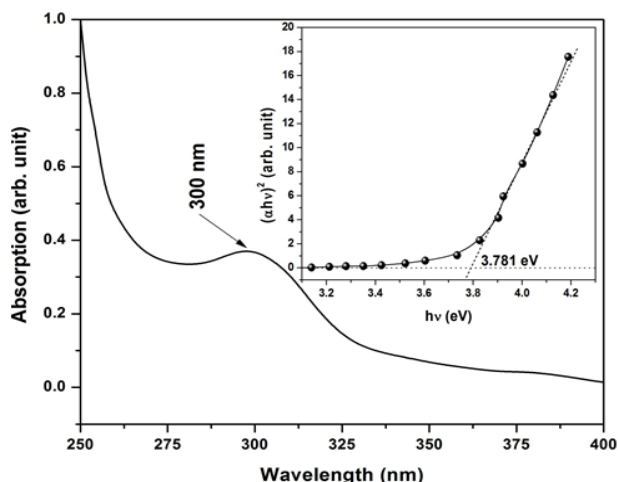


Fig. 5. UV-vis spectrum of flower-shaped ZnO (Inset: plot to determine direct band gap).

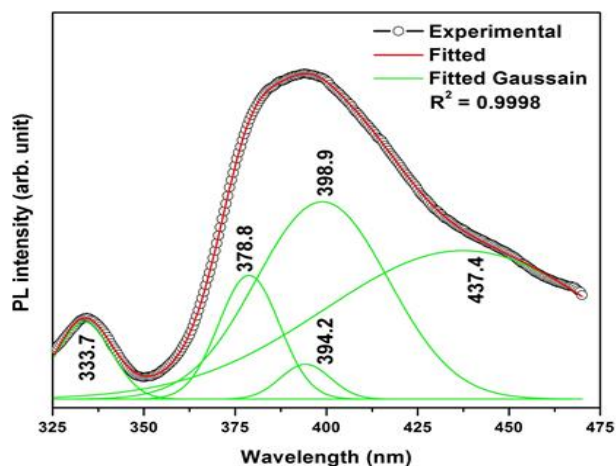


Fig. 6. Room temperature PL spectrum of flower-shaped ZnO (The Gaussian peaks marked in green colour at the bottom of the fitted curve which is marked in red colour).

The room temperature PL spectrum of flower-shaped ZnO NSs under excitation wavelength of 300 nm shown in Fig. 6 is obtained by deconvoluting the peaks with the help of Gaussian functions. The peak positions estimated are XC1=337.7 nm (3.72 eV), XC2=378.8 nm (3.27 eV), XC3=394.2 nm (3.15 eV), XC4=398.9 nm (3.11 eV) and XC5=437.4 nm (2.83 eV). The UV emission peaks (XC1, XC2, XC3 and XC4) observed in the sample corresponds to the near band-edge (NBE) emission of ZnO, which originated from the recombination of free excitons [24, 25]. The peak centered at XC2 is related to the band edge transition from conduction band to valance band and the transition associated with Zn vacancy in ZnO centered at XC4. The weak emission peak at XC5 corresponds to blue emission and is related to Zn interstitial defects [9, 26, 27].

In Fig. 7, the FTIR spectra of the sample are shown. The broad and intense peak at ~ 3390.8 cm^{-1} corresponds to O-H stretching vibrations of adsorbed water on the ZnO surface and the narrow peak at ~ 2959.2 cm^{-1} corresponds to C-H vibrations [21]. The peak at ~ 1652 cm^{-1} for pure PVP which correspond to

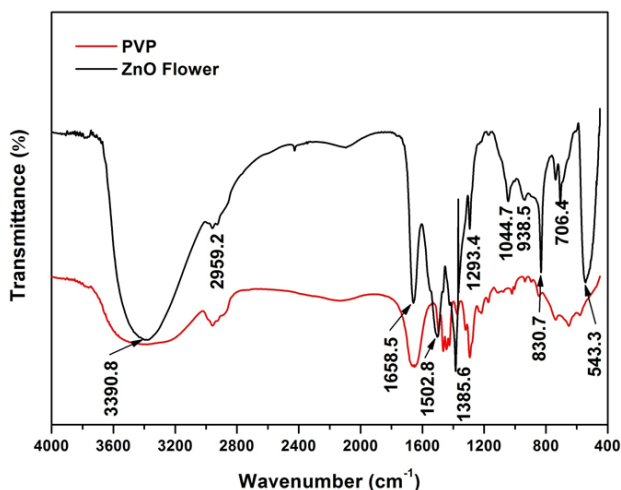


Fig. 7. FTIR spectra of PVP and flower-shaped ZnO.

C=O bond is shifted to peak at ~ 1658.5 cm^{-1} (C=O stretching) for PVP capped flower-like ZnO. This shift of infrared band for PVP is attributed to strong columbic interaction between ZnO and PVP matrix. Also, while the peaks at ~ 1385.6 to 1502.8 cm^{-1} , are produced as a result of CH₂ bends and deformation, that at ~ 1293.4 cm^{-1} corresponds to C-N stretching, confirming presence of organic groups of PVP and indicating that the PVP is preserved inside the ZnO [28]. Further, the peak observed at ~ 543.3 cm^{-1} is assigned to Zn-O stretching [29].

Conclusion

Flower-shaped ZnO is successfully synthesized at 60^oC using distilled water as a solvent by simple wet chemical method. The hexagonal phase of ZnO without any impurities is observed from XRD measurement. Analyses of SEM and TEM images confirmed flower-shaped ZnO originated from a center point of the flower having diameter $\sim 1.75 - 2.25$ μm . The particle sizes as observed from XRD and TEM have been found to be ~ 18.34 nm and less than ~ 25 nm respectively, which aggregate to flower-shaped ZnO nanostructures. FTIR analysis confirmed the interaction of ZnO and PVP molecule. In the PL study, the prepared sample shows NBE along with a weak blue emission. Since the sample shows absorption in the UV region at ~ 300 nm, which indicates blue shift of flower-shaped ZnO structure, therefore it may be concluded that the particles produced will surely find application in optical devices. It may be used for biological applications as well due to the rich surface properties observed. Using the innovative tools of nonlinear dynamical theory, we can not only predict such unusual behavior, but also use it for appropriate calibration in device fabrication, work proposed next as a logical follow-up.

Acknowledgements

The authors thank the P K Bora, Department of Physics & Astrophysics, Delhi University for FESEM measurement, and SAIF, NEHU, Shillong for TEM measurement; Department of Chemistry, Department of Applied Sciences and SAIF, Gauhati University for providing PL, UV-vis spectroscopy, FTIR spectroscopy and XRD measurements respectively.

Author's contributions

Conceived the plan: RKS, ES, MKD; Performed the experiments: RKS, MKD; Data analysis: RKS, ES, MKD; Wrote the paper: MKD. Authors have no competing financial interests.

Supporting information

Supporting informations are available from VBRI Press.

References

- Shabannia, R.; Abu-Hassan H; *Mater. Lett.* **2013**; *90*, 156. DOI: [10.1016/j.matlet.2012.09.037](https://doi.org/10.1016/j.matlet.2012.09.037)
- Xu, C.; Kim, D.; Chun, J.; Rho, K.; Chon, B.; Hong, S.; Joo, T.; *J. Phys. Chem. B.* **2006**; *110*; 21741. DOI: [10.1021/jp0631681](https://doi.org/10.1021/jp0631681)
- Xing, Y. J.; Xi, Z. H.; Zhang, X. D.; Song, J. H.; Wang, R. M.; Xu, J.; Xue, Z. Q.; Yu, D. P.; *Solid State Commun.* **2004**; *129*; 671. DOI: [10.1016/j.ssc.2003.11.049](https://doi.org/10.1016/j.ssc.2003.11.049)

4. Wang, X.; Ding, Y.; Summers, C. J.; Wang, Z. L.; *J. Phys. Chem. B***2004**, *108*, 8773.
DOI: [10.1021/jp048482e](https://doi.org/10.1021/jp048482e)
5. Chen, Z.; Shan, Z.; Li, S.; Liang, C. B.; Mao, S. X.; *J. Cryst. Growth***2004**, *265*, 482.
DOI: [10.1016/j.jcrysgro.2004.02.017](https://doi.org/10.1016/j.jcrysgro.2004.02.017)
6. Gao, S. Y.; Zhang, H. J.; Wang, X. M.; Deng, R. P.; Sun, D. H.; Zheng, G. L.; *J. Phys. Chem. B***2006**, *110*, 15847.
DOI: [10.1021/mn800353q](https://doi.org/10.1021/mn800353q)
7. Chakraborty, S.; Kole, A. K.; Kumbhakar, P.; *Mater. Lett.* **2012**, *67*, 362.
DOI: [10.1016/j.matlet.2011.10.018](https://doi.org/10.1016/j.matlet.2011.10.018)
8. Zhang, J.; Sun, L.; Yin, J.; Su, H.; Liao, C.; Yan, C.; *Chem. Mater.***2002**, *14*, 4172.
DOI: [10.1021/cm020077h](https://doi.org/10.1021/cm020077h)
9. Wei, X. Q.; Man, B. Y.; Liu, M.; Xue, C. S.; Zhuang, H. Z.; Yang, C.; *Physica B***2007**, *388*, 145.
DOI: [10.1016/j.physb.2006.05.346](https://doi.org/10.1016/j.physb.2006.05.346)
10. Gutul, T.; Rusu, E.; Condur, N.; Ursaki, V.; Goncarenco, E.; Vlazan, P.; *Beilstein Journal of Nanotech.***2014**, *5*, 402.
DOI: [10.3762/bjnano.5.47](https://doi.org/10.3762/bjnano.5.47)
11. Debanath, M. K.; Karmakar, S.; Borah, J. P.; *Adv. Sci. Eng. Med.* **2012**, *4(4)*, 306.
DOI: [10.1166/asem.2012.1163](https://doi.org/10.1166/asem.2012.1163)
12. Debanath, M.K.; Saha, R.K.; Borah, S.M.; Saikia, E.; Saikia, K.K.; *Adv. Mater. Proc.* **2018**, *3(1)*, 36.
DOI: [10.5185/amp.2018/721](https://doi.org/10.5185/amp.2018/721)
13. Saha, R.K.; Debanath, M.K.; Saikia, E.; Borah, V.V.; Saikia, K.K.; *Adv. Mater. Proc.* **2017**, *2(1)*, 26.
DOI: [10.5185/amp.2017/107](https://doi.org/10.5185/amp.2017/107)
14. Talebian, N.; Amininezhad, S.M.; Doudi, M.; *J. Photochem. Photobiol. B.* **2013**, *120*, 66.
DOI: [10.1016/j.jphotobiol.2013.01.004](https://doi.org/10.1016/j.jphotobiol.2013.01.004)
15. Debanath, M. K.; Karmakar, S.; *Mater. Lett.* **2013**; *111*, 116.
DOI: [10.1016/j.matlet.2013.08.069](https://doi.org/10.1016/j.matlet.2013.08.069)
16. Klug, H. P.; Alexander, L. E.; X-ray Diffraction Procedures for Polycrystalline and Amorphous Materials; Wiley: New York, 2nd ed., **1954**.
17. He, G.; Taowu, S.; Li, J.; *Funct. Mater. Lett.***2010**, *3*, 107.
DOI: [10.1142/S1793604710001044](https://doi.org/10.1142/S1793604710001044)
18. Komarneni, S.; Bruno, M.; Mariani, E.; *Mater. Res. Bull.***2000**, *35*, 1843.
DOI: [10.1016/S0025-5408\(00\)00385-8](https://doi.org/10.1016/S0025-5408(00)00385-8)
19. Wei, A.; Sun, X. W.; Xu, C. X.; Dong, Z. L.; Yang, Y.; Tan, S. T.; Huang, W.; *Nanotech.***2006**, *17*, 1740.
DOI: [10.1088/0957-4484/17/6/033](https://doi.org/10.1088/0957-4484/17/6/033)
20. Sheng, Y.; Jiang, Y.; Lan, X.; Wang, C.; Li, S.; Liu, X.; Zhong, H.; *J. Nanomater.***2011**.
DOI: [10.1155/2011/473629](https://doi.org/10.1155/2011/473629)
21. Krishnan, D.; Pradeep, T.; *J. Cryst. Growth***2009**, *311*, 3889.
DOI: [10.1016/j.jcrysgro.2009.06.019](https://doi.org/10.1016/j.jcrysgro.2009.06.019)
22. Manzoor, K.; Vadera, S. R.; N. Kumar, N.; Kutty, T. R. N.; *Solid State Commun.***2004**, *129(7)*, 469.
DOI: [10.1016/j.ssc.2003.11.012](https://doi.org/10.1016/j.ssc.2003.11.012)
23. Ghosh, G.; Naskar, M. K.; Patra, A.; Chatterjee, M.; *Optical Mater.* **2006**, *28(8-9)*, 1047.
DOI: [10.1016/j.optmat.2005.06.003](https://doi.org/10.1016/j.optmat.2005.06.003)
24. Kong, Y. C.; Yu, D. P.; Zhang, B.; *Appl. Phys. Lett.* **2001**, *78*, 407.
DOI: [10.1063/1.1342050](https://doi.org/10.1063/1.1342050)
25. Zeng, H. B.; Duan, G. T.; Li, Y.; Yang, S. K.; Xu, X. X.; Cai, W. P.; *Adv. Funct. Mater.***2010**, *20*, 561.
DOI: [10.1002/adfm.200901884](https://doi.org/10.1002/adfm.200901884)
26. Lin, B.; Fu, Z.; Jia, Y.; *Appl. Phys. Lett.* **2001**, *79*, 943.
DOI: [10.1063/1.1394173](https://doi.org/10.1063/1.1394173)
27. Kundu, S.; Sain, S.; Satpati, B.; Bhattacharyya, S. R.; Pradhan, S. K.; *RSC Adv.* **2015**, *5*, 23101.
DOI: [10.1039/c5ra01152c](https://doi.org/10.1039/c5ra01152c)
28. Zhang, T. R.; Lu, R.; Liu, X. L.; Zhao, Y. Y.; Li, T. J.; Yao, J. N.; *J. Solid. State Chem.***2003**, *172*, 458.
DOI: [10.1016/S0022-4596\(03\)00036-7](https://doi.org/10.1016/S0022-4596(03)00036-7)
29. Muthukumaran, S.; Gopalakrishnan, R.; *Optical Mater.***2012**, *34*, 1946.
DOI: [10.1016/j.optmat.2012.06.004](https://doi.org/10.1016/j.optmat.2012.06.004)